5

Doubly-fed Induction Generator Drives for Wind Power Plants

Balduino Rabelo and Wilfried Hofmann
Dresden University of Technology
Germany

1. Introduction

This chapter presents the theoretical basics of the electric power generation using doubly-fed induction drives in wind turbines. This type of drive is the most utilized in wind power plants nowadays. This is mainly due to its fast dynamic response and reduced power electronics on the rotor side. This latter aspect is responsible for less harmonic pollution in the network and reduced acquisition costs.
To begin with, the mathematical background required for comprehending the formulation used on electrical drives theory is repeated. Then the electromechanical energy conversion process in an electrical generator is explained, followed by a steady-state analysis of the induction machine. Subsequently, the doubly-fed induction generator and the network side circuit are introduced. Finally, active and power flow issues are discussed. The feasibility of reactive power production is in accordance with the new requirements from the power companies on wind energy converters and the degrees of freedom in its production allow for optimisation of the power losses.

2. Basic definitions

2.1 Complex space vectors

The space vector theory can be applied to all 3-phase system variables where these latter assume a complex vector representation. Besides the reduction from a 3 to a 2-phase system the suitable choice of a non-stationary coordinates system as a reference enables us to work with DC quantities. The representation simplifies, to a great extent, the coupling equations between both stator and rotor, as well as the computation of the 3-phase power. As an example the current space vector $\underline{i}$ representing the 3-phase symmetrical currents

$$i_a(t) = \hat{I}\cos(\omega_S t) \tag{1}$$

$$i_b(t) = \hat{I}\cos(\omega_S t - \frac{2\pi}{3}) \tag{2}$$

$$i_c(t) = \hat{I}\cos(\omega_S t - \frac{4\pi}{3}), \tag{3}$$

Source: Wind Power, Book edited by: S. M. Muyeen,
ISBN 978-953-7619-81-7, pp. 558, June 2010, INTECH, Croatia, downloaded from SCIYO.COM

where $\hat{I}$ is the current peak value and ω_S the angular frequency, can be determined as

$$\underline{i} = \frac{2}{3}\left[i_a(t) + \underline{a} i_b(t) + \underline{a}^2 i_c(t) \right] \tag{4}$$

where the operators $\underline{a} = e^{j\frac{2\pi}{3}}$ and $\underline{a}^2 = e^{j\frac{4\pi}{3}}$. The complex space vector can be related to the current instantaneous values by the expressions

$$i_a(t) = \Re\{\underline{i}\} + i_n \tag{5}$$

$$i_b(t) = \Re\{\underline{a}^2 \underline{i}\} + i_n \tag{6}$$

$$i_c(t) = \Re\{\underline{a}\underline{i}\} + i_n, \tag{7}$$

where i_n is the zero component of the current in a star connected system, as given by

$$i_n = \frac{1}{3}(i_a + i_b + i_c) \cdot \tag{8}$$

In a balanced symmetrical 3-phase system this term is not available.
The graphical representation of the vector addition of the single phase current components from expression (4) for i_a, $i_b > 0$ and $i_c < 0$ is depicted in figure 1. The $\alpha\beta$-coordinates frame is fixed on the stator with axis α on the same direction as that of the magnetic axis a. The dq-coordinates frame is rotating at an arbitrary angular speed

$$\omega_K = \frac{d\vartheta_K}{dt}, \tag{9}$$

where the phase displacement relative to the stator is a function of time

$$\vartheta_K(t) = \vartheta_0 + \int_0^t \omega_K dt \cdot \tag{10}$$

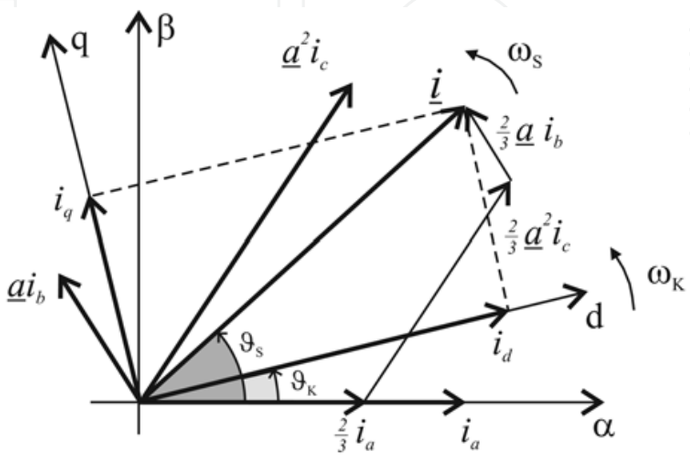

Fig. 1. Space vector in fixed and rotating coordinates

The current space vector $\underline{i}$ rotates at an angular speed

$$\omega_S = \frac{d\vartheta_S}{dt} \tag{11}$$

corresponding to the frequency of the 3-phase stator currents and can be represented as

$$\underline{i}^S = \underline{i}e^{j\vartheta_S}. \tag{12}$$

The complex exponential term performs the rotation of the space vector. Referring $\underline{i}$ to the rotating dq-frame require a coordinate transformation as follows

$$\underline{i}^K = \underline{i}e^{j(\vartheta_S - \vartheta_K)} = \underline{i}^S e^{-j\vartheta_K}. \tag{13}$$

The angular speed of the rotating coordinate system ω_K can be selected arbitrarily so that if $\omega_K = 0$ is chosen one gets a fixed coordinate system whose orientation will depend on the angle ϑ_0 in (10). If $\vartheta_0 = 0$, for example, one gets the $\alpha\beta$-coordinate system as a reference.
If ω_K is chosen to be equal the electrical rotor angular frequency

$$\omega = \frac{d\vartheta}{dt} = P_P\omega_m, \tag{14}$$

where P_P stands for the number of pole pairs and ω_m is the mechanical angular frequency of the rotor, the dq-coordinate system will be fixed on the rotor circuit.
If $\omega_K = \omega_S$ the difference angle $\vartheta_S - \vartheta_K$ is constant, i.e. the dq-coordinate frame rotates synchronously with the current space vector. Therefore, under steady state contitions the space vector $\underline{i}$ can be decomposed in 2 DC scalar components i_d and i_q as follows

$$i_d = \|\underline{i}\|\cos(\vartheta_S - \vartheta_K) \tag{15}$$

$$i_q = \|\underline{i}\|\sin(\vartheta_S - \vartheta_K), \tag{16}$$

where $\|\underline{i}\|$ is the bi-dimensional Euclidean norm of the space vector which gives the peak value of the phase current

$$\hat{I} = \|\underline{i}\| = \sqrt{i_d^2 + i_q^2}. \tag{17}$$

Therefore, i_d and i_q are the projections of $\underline{i}$ over the rotating coordinate system, as depicted in figure 1. Assuming the d-axis as real and the q-axis as imaginary a very useful complex notation for the space vectors can be derived

$$\underline{i} = i_d + ji_q. \tag{18}$$

2.1.1 Transformation operators.

Coordinate transformation is an operation used quite frequently in controlling modern electrical drives. The instantaneous 3-phase values are measured, sampled and given to the control algorithm at a rate ranging from a few to tens of kilohertz. If dq modeling is used,

transformations have to be carried out using the same rate, which is a burden for the processor. Hence, instead of using transcendental functions, coordinate transformations are derived in matrix form having trigonometric functions as elements. These latter are computed as truncated series or as look-up tables

Assuming a 3-phase system a matrix operator $\mathbf{T}_0$ that maps the column-vector $\mathbf{i}_{abc}$ containing the instantaneous values of the 3-phase currents as elements onto the column-vector $\mathbf{i}_{dq0}$, whose elements are the $dq0$ components, as follows

$$\mathbf{i}_{dq0} = \mathbf{T}_0 \mathbf{i}_{abc} \Rightarrow \begin{pmatrix} i_d \\ i_q \\ i_0 \end{pmatrix} = \mathbf{T}_0 \begin{pmatrix} i_a \\ i_b \\ i_c \end{pmatrix}. \tag{19}$$

After solving the equation above, one obtains the following matrix operator which defines the well-know Park transformation

$$\mathbf{T}_0 = \frac{2}{3} \begin{pmatrix} \cos(\omega_K t) & \cos(\omega_K t - \frac{2\pi}{3}) & \cos(\omega_K t - \frac{4\pi}{3}) \\ -\sin(\omega_K t) & -\sin(\omega_K t - \frac{2\pi}{3}) & -\sin(\omega_K t - \frac{4\pi}{3}) \\ 0.5 & 0.5 & 0.5 \end{pmatrix}. \tag{20}$$

The third line of the transformation matrix accommodates the zero-sequence component.

The back-transformation matrix from the $dq0$ to the abc system is accomplished by using the inverse of (20)

$$\mathbf{i}_{abc} = \mathbf{T}_0^{-1} \mathbf{i}_{dq0}, \tag{21}$$

where

$$\mathbf{T}_0^{-1} = \frac{3}{2} \mathbf{T}_0^T = \begin{pmatrix} \cos(\omega_K t) & -\sin(\omega_K t) & \frac{1}{2} \\ \cos(\omega_K t - \frac{2\pi}{3}) & -\sin(\omega_K t - \frac{2\pi}{3}) & \frac{1}{2} \\ \cos(\omega_K t - \frac{4\pi}{3}) & -\sin(\omega_K t - \frac{4\pi}{3}) & \frac{1}{2} \end{pmatrix}. \tag{22}$$

Other useful operations to the electrical drives theory are the partial transformations $\mathbf{T}_1$, between a 3 to a 2-phase stationary system, and $\mathbf{T}_2$, between the stationary to a rotating coordinate system, defined as follows

$$\mathbf{i}_{\alpha\beta 0} = \mathbf{T}_1 \mathbf{i}_{abc} \Rightarrow \mathbf{T}_1 = \frac{2}{3} \begin{pmatrix} 1 & -\frac{1}{2} & -\frac{1}{2} \\ 0 & \frac{\sqrt{3}}{2} & -\frac{\sqrt{3}}{2} \\ \frac{1}{2} & \frac{1}{2} & \frac{1}{2} \end{pmatrix} \tag{23}$$

$$\mathbf{i}_{dq0} = \mathbf{T}_2 \mathbf{i}_{\alpha\beta 0} \Rightarrow \mathbf{T}_2 = \begin{pmatrix} \cos(\omega_K t) & \sin(\omega_K t) & 0 \\ -\sin(\omega_K t) & \cos(\omega_K t) & 0 \\ 0 & 0 & 1 \end{pmatrix} \tag{24}$$

The respective back-transformations are found by inverting the matrices (23) and (24)

$$\mathbf{i}_{abc} = \mathbf{T}_1^{-1} \mathbf{i}_{\alpha\beta 0} \Rightarrow \mathbf{T}_1^{-1} = \begin{pmatrix} 1 & 0 & 1 \\ -\frac{1}{2} & \frac{\sqrt{3}}{2} & 1 \\ -\frac{1}{2} & -\frac{\sqrt{3}}{2} & 1 \end{pmatrix} \tag{25}$$

$$\mathbf{i}_{\alpha\beta 0} = \mathbf{T}_2^{-1} \mathbf{i}_{dq} \Rightarrow \mathbf{T}_2^{-1} = \begin{pmatrix} \cos(\omega_K t) & -\sin(\omega_K t) & 0 \\ \sin(\omega_K t) & \cos(\omega_K t) & 0 \\ 0 & 0 & 1 \end{pmatrix} \tag{26}$$

2.2 Electrical power computation

The computation of the electrical power is an extensive subject and the definitions according to the DIN 40110 standard *Wechselstromgrössen - Zweileiter Stromkreise* (1994) used throughout the text will be explained here. The matter is addressed in detail in the above mentioned norm and in other literature Späth (2000).

2.2.1 Non-sinusoidal wave forms.

Due to the rectangular voltage wave forms in power converters output and their effects on voltage drops and currents in connected circuits, it is necessary to have suitable mathematical tools in order to analyse these kind of phenomena. Thus, for any non-sinusoidal periodic wave form that submit to the Dirichlet conditions there exists a convergent Fourier series. Thus, the Fourier series representation of any periodic single phase voltage and current wave forms can be written as

$$u(t) = U_0 + \sum_{\mu=1}^{\infty} \hat{U}_\mu \cos(\mu\omega t + \alpha_\mu) \tag{27}$$

$$i(t) = I_0 + \sum_{\nu=1}^{\infty} \hat{I}_\nu \cos(\nu\omega t + \beta_\nu), \tag{28}$$

where U_0 and I_0 are the DC components and the summations represent the time periodic components $\tilde{u}(t)$ and $\tilde{i}(t)$, i.e., the AC components of $u(t)$ and $i(t)$.
The instantaneous power that is being transferred by the voltage and current is given by

$$p(t) = u(t)i(t). \tag{29}$$

By definition the active power P is the mean value of the instantaneous power over the time period of the fundamental frequency. Substituting the expressions (27) and (28) on (29), after some development one arrives at

$$P = \overline{p}(t) = U_0 I_0 + \frac{1}{2}\sum_{\mu=1}^{\infty}\hat{U}_\mu \hat{I}_\mu \cos(\alpha_\mu - \beta_\mu)\cdot \tag{30}$$

From the equation above one observes that only the *DC* and the components with same frequency contribute to the average active power. If only the *DC* components are available, the active power is given solely by the first equation term, whereas if there are no such components the summation of the voltage and current products with the same harmonic order define the power. Considering no DC components, the fundamental components of sinusoidal voltage and current are given by

$$u_1(t) = u(t) - \sum_{\mu=2}^{\infty}\hat{U}_\mu \cos(\mu\omega t + \alpha_\mu) = \hat{U}_1 \cos(\omega t + \alpha_1) \tag{31}$$

$$i_1(t) = i(t) - \sum_{\nu=2}^{\infty}\hat{I}_\nu \cos(\nu\omega t + \beta_\nu) = \hat{I}_1 \cos(\omega t + \beta_1)\cdot \tag{32}$$

The harmonic components $\tilde{u}(t)$ and $\tilde{i}(t)$ denoted by the summations on both equations above are considered distortions of the fundamental sinusoidal wave forms

$$u(t) = u_1(t) + \tilde{u}(t), \quad \tilde{u}(t) = \sum_{\mu=2}^{\infty}\hat{U}_\mu \cos(\mu\omega t + \alpha_\mu) \tag{33}$$

$$i(t) = i_1(t) + \tilde{i}(t), \quad \tilde{i}(t) = \sum_{\nu=2}^{\infty}\hat{I}_\nu \cos(\nu\omega t + \beta_\nu)\cdot \tag{34}$$

2.2.2 Nature of reactive power.

The standard *Wechselstromgrössen - Zweileiter Stromkreise* (1994) defines the reactive power as the mean value of the product of the voltage delayed by a quarter of its fundamental period times the current

$$Q = \overline{q}(t) = \frac{1}{T}\int_t^{T+t} u(t - \frac{T}{4})i(t)dt, \quad T = \frac{2\pi}{\omega}\cdot \tag{35}$$

It represents the amount of energy that cannot be converted being exchanged between electric and magnetic fields, i.e. source and load, over the time.

More general discussion about the nature of the electrical powers will be avoided at this point. For the purposes of this work the definitions presented above are considered sufficient. Furthermore, this is a very extensive matter that is once and again treated in the literature Späth (2000). Unsymmetrical systems requiring determination of positive, negative and zero sequences will also not be dealt here, since faulty conditions are not going to be treated.

2.2.3 Complex power.

Taking equations (15) to (18) for the currents one can derive the following expressions for the voltage and current effective complex vectors

$$\underline{U} = U(\cos\varphi_u + j\sin\varphi_u) = Ue^{j\varphi_u} \tag{36}$$

$$\underline{I} = I(\cos\varphi_i + j\sin\varphi_i) = Ie^{j\varphi_i}, \tag{37}$$

By multiplying (36) by the complex conjugate of (37) yields

$$\underline{U}\cdot\underline{I}^* = UIe^{j(\varphi_u-\varphi_i)} = UI\cos\varphi + jUI\sin\varphi\cdot \tag{38}$$

Thus, the complex power $\underline{S}$ can be defined as

$$\underline{S} = \underline{U}\cdot\underline{I}^* = P + jQ\cdot \tag{39}$$

The same can be deduced for the 3-phase power. Furthermore, due to the fact that in steady-state, the instantaneous values equal the average values, and the powers can be computed using the instantaneous values of the complex vectors as follows

$$\underline{S} = P + jQ = \frac{3}{2}\{\underline{u}\cdot\underline{i}^*\}, \tag{40}$$

where the average active and reactive powers are the respective real and imaginary parts of (40). The instantaneous active and reactive power values can be written as functions of the scalar components of voltages and currents on the *dq*-axis as follows

$$p(t) = \frac{3}{2}\Re\{\underline{u}\cdot\underline{i}^*\} = \frac{3}{2}\{u_d i_d + u_q i_q\} \tag{41}$$

$$q(t) = \frac{3}{2}\Im\{\underline{u}\cdot\underline{i}^*\} = \frac{3}{2}\{u_q i_d - u_d i_q\}\cdot \tag{42}$$

3. Electric generators

The next step in energy conversion in a wind turbine is the transformation of the mechanical energy of the rotating masses into electrical energy by means of an electrical machine. To produce the required electromagnetic torque as a reaction of the electrical subsystem to the mechanical driving torque in order to absorb the input mechanical energy, the generator must be excited, i.e., magnetic energy must be available in the air-gap between stator and rotor. Therefore, the magnetic field is responsible for coupling the electrical and mechanical subsystems and consequently reactive power is required in order to magnetise the generator. The exact way in which the electromechanical energy conversion process takes place in a given electrical machine depends on its construction. The distribution of the magnetic induction on the air-gap depends on its geometry, on the distribution of the winding conductors and on the iron's magnetic characteristics. Although the detailed theoretical deduction of the rotating field electrical machines is usually found in the literature Leonhard (1980); Lipo (1995); Müller (1977) the basics of this in the case of an induction machine is repeated here for a completion of the text.

3.1 Induction machine.

Wound rotor induction and synchronous machines are the mostly used generator types in wind power plants. Induction machines are very well known, and one of the most employed types in several areas, due mainly to its robustness, power-to-volume ratio and relative low cost. However, induction machines do not possess separated field circuits as do synchronous or DC machines. These are lumped together with the armature circuit in the stator windings so that a decoupled control of torque and flux, or active and reactive powers, requires some mathematical treatment of the machine model. However, this is no longer a drawback thanks to the development of the power electronics and microprocessors of the last 20 years. Today, high dynamics and reliable machine drives can be assembled with relative low cost.

There are basically two types of induction machines, the squirrel cage and the wound rotor. In squirrel cage induction machines the rotor circuit is made up of aluminum or copper bars cast in the rotor iron and short-circuited by non-accessible end-rings. The required magnetization is normally drawn from outside through the stator windings. This can be accomplished using a capacitor bank parallel to the machine terminals in a self-excited scheme or feeding the stator with an inverter or by simply connecting the machine terminals to the grid supply. The squirrel cage induction machine is currently the industry's horse power.

The construction of the wound rotor induction machine is likely the squirrel cage one. Instead of short-circuited bars, the windings in the rotor slots end up on copper slip-rings mounted to the shaft. The connection to the static part is accomplished through fixed carbon brushes that make pressure contact by means of adjustable springs to the turning rings. In this way the rotor circuit is also available to external connections like additional rotor resistors for startup, speed control, slip power recovery schemes or controlled voltage and frequency sources. The wound rotor induction machine was often used as a rotating frequency converter in the past but became obsolete upon the development of semiconductors and static converters. Its renaissance took place first on pump storage hydroelectric power plants, where high power variable speed drives that operate as motor and generator were required. The reduced power converters needed in the speed control within a slip power recovery scheme makes the wound rotor machine very attractive. Later on, it established a place on the market as a doubly-fed generator for wind power plants.

3.1.1 Rotating field electrical machines

Assuming a 2–pole induction machine having 3–phase symmetrical windings a – a', b – b' and c–c' with the respective magnetic axis a, b and c 120° spatially separated from each other, mounted on the stator and on the rotor. The stator windings are fed by symmetrical 3–phase currents like (5) to (7). The rotor is assumed cylindrical and the air-gap radial dimension g constant, i.e., eccentricity and slot harmonics as well as end-winding effects are not taken into account. Permeability of the iron is much greater than that of the air, so that the flux density is concentrated on the air-gap crossings and saturation effects in the iron can be neglected.

3.1.2 Steady-state equivalent circuit.

Based on the self inductances and on the flux linkages, the voltage equations under steady-state conditions can be written in complex form as follows

$$\underline{u}_S = R_S \underline{i}_S + j\omega_S \underline{\Psi}_S \tag{43}$$

$$\underline{u}'_R = R'_R \underline{i}'_R + j\omega_R \underline{\Psi}_R, \tag{44}$$

where ω_R is the slip frequency and the flux linkages are given by

$$\underline{\Psi}_S = L_S \underline{i}_S + L_m \underline{i}'_R \tag{45}$$

$$\underline{\Psi}_R = L'_R \underline{i}'_R + L_m \underline{i}_S . \tag{46}$$

From the direct proportionality of the flux density to the current vectors the magnetizing current vector i_μ can be computed as the vector addition of the stator and rotor current vectors related to the stator side as follows

$$\underline{i}_\mu = \underline{i}_S + (\frac{N_R}{N_S})\underline{i}_R = \underline{i}_S + \underline{i}'_R, \tag{47}$$

where N_S and N_R are the stator and rotor number of turns. By substituting the imaginary coefficients with the respective mutual and leakage inductive reactances

$$X_m = \omega_S L_m \tag{48}$$

$$X_\sigma = \omega_S L_\sigma \tag{49}$$

and the magnetising current (47) in the voltage and flux linkage equations yields

$$\underline{u}_S = R_S \underline{i}_S + jX_{\sigma_s} \underline{i}_S + jX_m \underline{i}_\mu \tag{50}$$

$$\frac{\underline{u}'_R}{s} = \frac{R'_R}{s} \underline{i}'_R + jX'_{\sigma_R} \underline{i}'_R + jX_m \underline{i}_\mu \tag{51}$$

where the slip is defined as $s = \frac{\omega_R}{\omega_S}$.

Departing from the magnetic induction resulting from the superposition of the stator and rotor magnetic induction waves and from the rotation induced voltage, the main flux linkage vector $\underline{\Psi}_m$ induces the stator and rotor internal voltages, respectively $\underline{e}_S$ and $\underline{e}'_R$

$$\underline{e}_S = -j\omega_S \underline{\Psi}_m = -j\omega_S L_m \underline{i}_\mu, \tag{52}$$

$$\underline{e}'_R = -js\omega_S \underline{\Psi}_m = -js\omega_S L_m \underline{i}_\mu . \tag{53}$$

These expressions show that both stator and rotor induced voltages are related by the slip s as follows

$$\underline{e}'_R = (\frac{N_R}{N_S})\underline{e}_R = s\underline{e}_S . \tag{54}$$

The complex voltage drop over the stator winding can be determined by substituting (52) in the voltage equation (50).

$$\underline{u}_S = R_S \underline{i}_S + jX_{\sigma_S} \underline{i}_S - \underline{e}_S \cdot \tag{55}$$

Similarly, by substituting (53) in the rotor voltage equation (51) and multiplying both sides of the equation by s gives

$$\underline{u}'_R = R'_R \underline{i}'_R + jsX'_{\sigma_R} \underline{i}'_R - e'_R \cdot \tag{56}$$

The single phase equivalent circuit of the induction machine based on equations (50) and (51) as well as on equations (55) and (56) is depicted in figure 2.

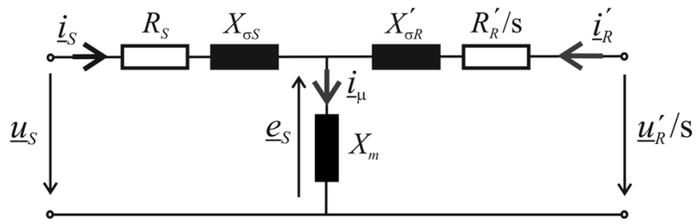

Fig. 2. Equivalent circuit of the induction machine

The constant mains voltage drives the stator current and the machine magnetisation. The resulting rotor induced voltage has to be counter-balanced by means of the voltage drop over the rotor impedance and by the terminal voltage. The interaction of the stator and rotor currents, due to the superposition of the magnetic induction waves, results in the magnetizing current as shown in expression (47).

Taking the equation (56) and considering short-circuited rotor bars as in the cage induction machine, i.e., $\underline{u}'_R = 0$ yields

$$\underline{0} = R'_R \underline{i}'_R + jsX'_{\sigma_R} \underline{i}'_R - e'_R \cdot \tag{57}$$

In this particular case the complex voltage drop over the rotor impedance must equal the rotor induced voltage. Figure 3 shows the space vector diagram of the stator and rotor values for a squirrel cage induction machine.

The stator power factor angle φ_S is defined as the angle between the terminal voltage and the current vectors. The rotor power factor angle φ_R between the rotor induced voltage and rotor current vectors is a function of the rotor parameters and of the slip given by

$$\varphi_R = \arctan\left(s \frac{X_{\sigma_R}}{R_R}\right) \cdot \tag{58}$$

From this expression and from figure 3, one finds that by increasing the slip, i.e., loading the machine, results in an increase in the rotor power factor angle, theoretically up to $\varphi_R = \pi / 2$ for $s = \infty$, and a decrease on the stator power factor angle φ_S. Towards no-load condition the stator power factor decreases to nearly zero while the rotor power factor is nearly unity.

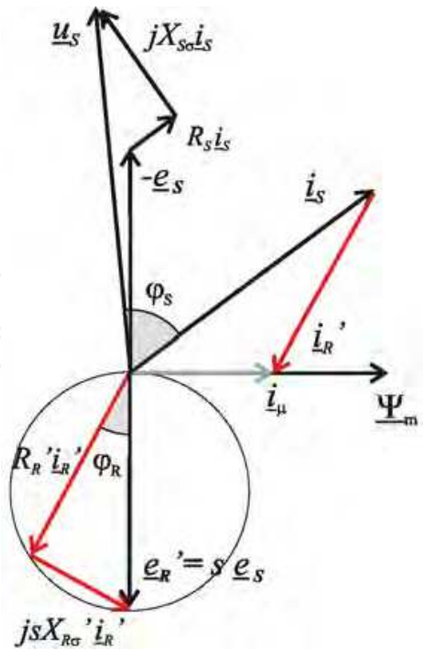

Fig. 3. Current space vectors in an induction machine

3.2 Energy and power balance.

In a physical system the variation of stored magnetic energy plus losses accounts for the difference between the input and the output energy variations

$$dW_{mag} + dW_{loss} = dW_{ele} - dW_{mech}, \tag{59}$$

where W is the energy, the subscripts *mag*, *ele* and *mech* denote its magnetic, electric and mechanical forms, respectively, and *loss* stands for inherent process losses, i.e., the energy converted into heat. The electromechanical energy conversion process is based on the energy conservation principle pointed out by this expression.

To keep a constant excitation level, i.e., maintaining the amount of magnetic energy constant, any variation in the input energy to the system must be followed by a variation in the system output thereby accounting for the process losses as shown in the following equation

$$dW_{loss} = dW_{ele} - dW_{mech}, \tag{60}$$

A detailed description of the electromechanical energy conversion process can be found in the literature Müller (1977).

As power is defined as the rate of change of energy

$$p(t) = \frac{dW}{dt} \Rightarrow dW = p(t)dt, \tag{61}$$

equation (60) can be rewritten more explicitly as follows

$$p_{loss}dt = uidt - m_e\omega_m dt, \tag{62}$$

where p_{loss} represents the instantaneous power losses, u and i stand for terminal voltage and current and m_e and ω_m are the electromagnetic torque and the mechanical angular speed of the shaft, respectively.
Defining the average power as the average energy exchange over the time interval Δt, the equation (62) takes the form of a difference equation

$$P_{loss}\Delta t = P_{ele}\Delta t - P_{mech}\Delta t, \tag{63}$$

where P_{ele} and P_{mech} are the average electrical an mechanical powers during Δt, respectively. Eliminating the time in the expression (63) leads to the power balance equation

$$P_{loss} = P_{ele} - P_{mech}\,. \tag{64}$$

3.2.1 Active power.

Considering the motor operation of the induction machine as the positive direction for the active power flow, the power balance equation (64) for steady-state can be assumed. The power losses will be defined and situated according to their cause and where they take place. Therefore, stator and rotor copper losses as well as the mechanical losses due to friction and windage on the shaft will be presented herein. In order to do so, intermediary power values in different locations are defined like the air-gap power, the rotor input power on the rotor terminals and the internal mechanical power. Iron losses will be neglected here for the sake of simplicity and explained later, when they will be taken into account in the optimization procedure.
The stator input instantaneous electrical power p_S is computed as shown in (41) using equation (55)

$$p_S = \frac{3}{2}\Re\{\underline{u}_S\underline{i}_S^*\} = \frac{3}{2}\Re\{R_S\underline{i}_S\underline{i}_S^* + jX_{\sigma_S}\underline{i}_S\underline{i}_S^* - \underline{e}_S\underline{i}_S^*\}\,. \tag{65}$$

The first term in (65) accounts for the energy dissipated as heat over the stator windings resistance resulting in the stator copper losses

$$P_{Cu_S} = \frac{3}{2}R_S\hat{I}_S^2\,. \tag{66}$$

By subtracting (66) from (65) results in the air-gap power p_g given by the third term in (65), since the second term is a pure imaginary number

$$p_g = p_S - P_{Cu_S} = -\frac{3}{2}\Re\{\underline{e}_S\underline{i}_S^*\}\,. \tag{67}$$

The power balance for the rotor circuit can be found in the following relation

$$p_g + p_R = p_{mech} + P_{Cu_R}\,, \tag{68}$$

where p_R is the input rotor power on the slip-ring terminals, p_{mech} is the internal mechanical power and P_{CuR} stands for the rotor copper losses. The input rotor power is computed in much the same was as the stator input power. From the voltage equation (56)

$$p_R = \frac{3}{2}\Re\{\underline{u}'_R \underline{i}'^*_R\} = \frac{3}{2}\Re\{R'_R \underline{i}'_R \underline{i}'^*_R + jsX'_{\sigma_R} \underline{i}'_R \underline{i}'^*_R - \underline{e}'_R \underline{i}'^*_R\}. \tag{69}$$

By analogy to the stator, the rotor copper losses are given by

$$P_{Cu_R} = \frac{3}{2} R'_R \hat{I}'^2_R. \tag{70}$$

On substituting (69) and (70) in (68) yields

$$p_{mech} - p_g = -\frac{3}{2}\Re\{\underline{e}'_R \underline{i}'^*_R\}. \tag{71}$$

Application of the current relation (47) and the induced voltage relation (54) in (71) allows for the following development

$$p_{mech} - p_g = -\frac{3}{2}\Re\{s\underline{e}_S(\underline{i}_\mu - \underline{i}_S)^*\} = \frac{3}{2}s\Re\{\underline{e}_S \underline{i}^*_S\}. \tag{72}$$

The internal mechanical power can then be expressed as a function of the air-gap power and of the slip

$$p_{mech} - p_g = -sp_g \Rightarrow p_{mech} = (1-s)p_g. \tag{73}$$

Taking the equation (73) and substituting it in (68) leads to the following result

$$p_R = -sp_g + P_{Cu_R}. \tag{74}$$

From (73) and (74) one may conclude that the distribution of the power transferred through the air-gap depends on the slip. In relation to the wound rotor machine, it translates into the ratio between the rotor and stator active powers

$$s = -\frac{p_R - P_{Cu_R}}{p_S - P_{Cu_S}}. \tag{75}$$

Equation (75) is a basic relation that fosters an understanding on how the wound rotor induction machine operates. The negative sign comes from the motor convention used.
For motoring condition ($P_S > 0$) power is fed from the rotor ($P_R < 0$) under sub-synchronous operation ($s > 0$) and from the mains to the rotor ($P_R > 0$) under super-synchronous operation ($s < 0$). For generating condition ($P_S < 0$) power is fed to the rotor under sub-synchronous operation and from the rotor to the mains under super-synchronous operation. These results are summarised in table 1.
In the case of a squirrel cage induction machine, where the power on the rotor terminals equals zero, the slip provides the relation between the rotor copper losses and the air-gap power. In other words, the amount of air-gap power given by the slip must cover the rotor copper losses

$$s = \frac{P_{Cu_R}}{p_g}. \tag{76}$$

Operating Condition	Motor ($P_S > 0$)	Generator ($P_S < 0$)
Sub-synchronous ($s > 0$)	$P_R < 0$	$P_R > 0$
Super-synchronous ($s < 0$)	$P_R > 0$	$P_R < 0$

Table 1. Power flow under different operating conditions

The mechanical losses account for the friction and windage losses during machine operation. The first is a function of the squared angular speed while the second is a function of the cubic angular speed. The separation of these losses is a complex task as well as the determination of the respective proportionality factors. Therefore, a single friction coefficient proportional to the power 2.5 of the angular speed will be considered

$$p_f = B_G \omega_m^{2.5} \cdot \tag{77}$$

And on being subtracted from the internal mechanical power, this results the output mechanical power delivered to the load by the rotating shaft p_{load}

$$p_{load} = p_{mech} - p_f \cdot \tag{78}$$

3.2.2 Reactive power.

The reactive power flow is responsible for the maintenance of the magnetic energy stored in the air-gap as well as for the building up of the flux linkages required for the energy conversion process.

The reactive power flowing through the stator terminals is computed using (42) on (55) and results in the amount of reactive power required for building up the stator flux linkage $\underline{\Psi}_S$

$$q_S = \frac{3}{2}\Im\{\underline{u}_S \underline{i}_S^*\} = \frac{3}{2}\Im\{R_S \underline{i}_S \underline{i}_S^* + jX_{\sigma_S} \underline{i}_S \underline{i}_S^* - \underline{e}_S \underline{i}_S^*\} \cdot \tag{79}$$

From equation (79) one sees that only the second and third terms are reactive powers; the second term being responsible for creating the stator leakage flux $\underline{\Psi}_{\sigma S}$

$$q_{\sigma_S} = \frac{3}{2}\Im\{jX_{\sigma_S} \underline{i}_S \underline{i}_S^*\} \tag{80}$$

and its average value is then

$$Q_{\sigma_S} = \frac{3}{2} X_{\sigma_S} \hat{I}_S^2 \cdot \tag{81}$$

The remaining term in (79) represents the one which actually contributes to the magnetization of the machine.

$$q_S - q_{\sigma_S} = -\frac{3}{2}\Im\{\underline{e}_S \underline{i}_S^*\} = -\frac{3}{2}\Im\{\underline{e}_S(\underline{i}_\mu - \underline{i}'_R)^*\}. \tag{82}$$

According to (47), (82) goes into

$$q_S - q_{\sigma_S} = -\frac{3}{2}\Im\{\underline{e}_S \underline{i}_\mu^*\} + \frac{3}{2}\Im\{\underline{e}_S \underline{i}'^*_R\}. \tag{83}$$

The first part of the equation (83) stands for the actual amount of reactive power involved in building up the mutual flux linkage $\underline{\Psi}_m$ and according to (52), the magnetising reactive power can be written as follows

$$q_m = -\frac{3}{2}\Im\{\underline{e}_S \underline{i}_\mu^*\} = \frac{3}{2}\Im\{j\omega_S L_m \underline{i}_\mu \underline{i}_\mu^*\}. \tag{84}$$

The average magnetising power can then be written as

$$Q_m = \frac{3}{2} X_m \hat{I}_\mu^2. \tag{85}$$

The second part stands for the contribution of the rotor current vector towards magnetisation, and if one defines it as in Vicatos & Tegopoulos (1989) as the amount of reactive power being delivered to the air-gap

$$q_g = \frac{3}{2}\Im\{\underline{e}_S \underline{i}'^*_R\}, \tag{86}$$

the stator reactive power can be expressed as follows

$$q_S = q_{\sigma_S} + q_m + q_g. \tag{87}$$

Analogously to the stator side the rotor reactive power is the imaginary part of the apparent power in the rotor terminals that contributes to building up the rotor flux linkage $\underline{\Psi}_R$

$$q_R = \frac{3}{2}\Im\{\underline{u}_R \underline{i}'^*_R\} = \frac{3}{2}\Im\{R'_R \underline{i}'_R \underline{i}'^*_R + jsX'_{\sigma_R} \underline{i}'_R \underline{i}'^*_R - \underline{e}'_R \underline{i}'^*_R\}. \tag{88}$$

On analysing equation (88) one notices that the first term is a real number whereas the second stands for the reactive power required for building up the rotor leakage flux $\underline{\Psi}_{\sigma R}$

$$q_{\sigma_R} = \frac{3}{2}\Im\{jsX'_{\sigma_R} \underline{i}'_R \underline{i}'^*_R\}. \tag{89}$$

The rotor average reactive leakage power is given by

$$Q_{\sigma_R} = \frac{3}{2} sX'_{\sigma_R} \hat{I}'^2_R. \tag{90}$$

The third term is, similarly to the stator side in (83), a contribution of the rotor side to the machine magnetisation. Applying the induced voltage relation (54) and substituting the expression (86) yields

$$q_R - q_{\sigma_R} = -\frac{3}{2}\Im\{\underline{e}'_R \underline{i}'^*_R\} = -s\frac{3}{2}\Im\{\underline{e}_S \underline{i}'^*_R\} = -sq_g \,. \tag{91}$$

From equations (87) and (91) the following relation between stator and rotor reactive powers can be found

$$q_R - q_{\sigma_R} = -s(q_S - q_{\sigma_S} - q_m) \Rightarrow s = -\frac{q_R - q_{\sigma_R}}{q_S - q_{\sigma_S} - q_m} \,. \tag{92}$$

It can be concluded that the reactive powers on the stator and rotor sides are related by the slip, similarly to the active powers except by the reactive power required by the magnetisation.

3.3 The doubly fed induction generator

One of the preferable solutions employed as wind turbine generator is the wound rotor induction machine with the stator windings directly connected to the network and rotor windings connected to controllable voltage source through the slip-rings, also known as the doublyfed induction generator (DFIG), the object of this work. As already mentioned, one of the most attractive features of this drive is the required power electronics converter rated part of the generators nominal power, reducing the acquisition costs, inherent losses and harmonic pollution as well as volume.

The other most employed type of drive that shares the market with the DFIG is the gear-less high pole-numbered synchronous generator (SG). It is also an elegant and successful solution for the wind energy branch. The stator windings present high number of poles enabling the generator to turn with mechanical speeds of the same order of the turbine rotor. Thus there is no need for a gear-box and the generator shaft is directly connected to the turbine axis.

However, this drive requires a full rated power electronics converter between the stator and the grid in order to convert the generated variable voltage and frequency to the net constant values. This latter assumption, allied to the fact that the machine requires a very large diameter to accommodate the high number of poles, makes the manufacturing and assembling process costly. Furthermore, the drive train and generator must be dimensioned in order to experience the turbine torque peaks at this speed range. On the other hand, the fast turning DFIG, due to its small number of poles, experiences reduced torque values compared to the gear-less SG and is produced in series by several manufacturers, since it is not a particularly costly process.

In addition, the DFIG can be operated as a synchronous machine, in that it is magnetized through the rotor, but has the advantage of not having the stiff torque versus speed characteristics. In this way it is possible to ”slip” over the synchronous speed, thus avoiding mechanical and electrical stresses to the drive train and network. In the synchronous operation of the DFIG the resulting magnetic induction vector direction is not coupled to the rotor position as it is in the synchronous machine (due to the construction of a DC exciting circuit or permanent magnet on the rotor). Neglecting the nut harmonic effects and considering concentrated windings, feeding 3-phase currents with slip frequency to the rotor windings, not only the amplitude also the position of the rotor field vector can be varied synchronously with the stator field vector, independently of the rotor position or

speed. In other words, active and reactive power, i.e. electromagnetic torque and excitation, can be controlled decoupled from each other and from rotor angle position Leonhard (1980). For the reasons pointed out above, the DFIG is one of the most used generator types in MW class wind power plants according to statistical figures disclosed in Germany recently Rabelo & Hofmann (2002). There is also an increasing tendency to employ the DFIG in upcoming higher powered turbines. Other promising variants that do not require the power electronics converter using the synchronous generator combined with a hydrodynamic controlled planetary gear in order to keep the synchronous speed left recently the prototype phase and are being already manufactured in series Rabelo et al. (2004).

3.3.1 Simplified analysis.

In order to explain the operation of a wound rotor induction machine, some simplifications on the steady-state circuit will be provided. This is merely for better comprehension of the machine operation and do not invalidate the theory presented to this point. Deviations from the complete original model will be pointed out.

Neglecting the voltage drop over the stator winding resistance and the stator leakage reactance in the equation (55), which is a reasonable assumption in the case of high powered machines, yields

$$\underline{u}_S = -\underline{e}_S = j\omega_S \underline{\Psi}_m = j\omega_S L_m \underline{i}_\mu \,. \tag{93}$$

As a result, the induced voltage vector $\underline{e}_S$ has the same amplitude and opposite direction of the terminal voltage vector $\underline{u}_S$. And the magnetising flux vector $\underline{\Psi}_m$, as well as the magnetizing current, $\underline{i}_\mu$ lags the terminal voltage by 90°.

These first assumptions lead to a reduction of the machine's equivalent circuit as presented in figure 4.

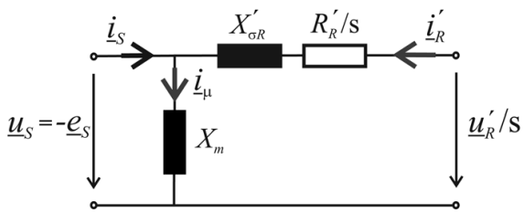

Fig. 4. Simplified equivalent circuit of the induction machine.

The new simplified voltage equation for this circuit is easily deduced

$$\underline{u}'_R = R'_R \underline{i}'_R + jsX'_{\sigma_R} \underline{i}'_R + s\underline{u}_S, \tag{94}$$

as well as the rotor current

$$\underline{i}'_R = \frac{\underline{u}'_R - s\underline{u}_S}{R'_R + jsX'_{\sigma_R}} \,. \tag{95}$$

With regard to what happens with the additional rotor resistance, a controllable voltage source applies similar voltage drop over the resistance in the rotor terminals. The basic idea is to counter balance the induced voltage by different slip values applying suitable values of

the voltage to the rotor terminals, i.e. the slip-rings, in order to control speed and/or torque so as to keep the rotor current under acceptable values. Hence, the voltage source ceiling value depends on the desired operating range. For different rotor voltage values, different base or synchronous speeds are also given. The base slip s_0 can be found by setting the rotor current vector to zero for a respective rotor voltage on the equation (95)

$$\underline{u}'_{R0} = s_0 \underline{u}_S \Rightarrow s_0 = \frac{\underline{u}'_{R0}}{\underline{u}_S}. \tag{96}$$

The admissible values for the rotor current normally take place over the speed range for a short-circuited rotor. Therefore, the voltage difference on the numerator of equation (95) must lie within the same range of the voltage drop in the rotor windings for the machine with short-circuited rotor, as shown in the figure 5.

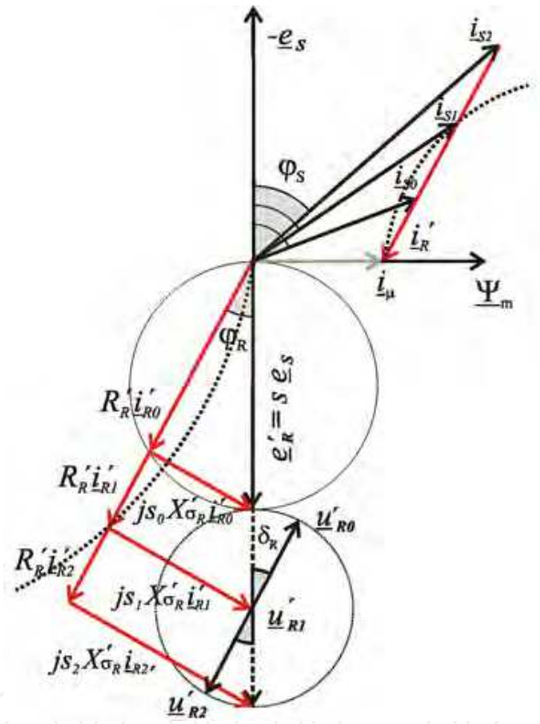

Fig. 5. Variation of the rotor voltage

The diagram of the figure 5 presents the variation of the rotor terminal voltage along three values $\underline{u}'_{R0}$, $\underline{u}'_{R1}$ and $\underline{u}'_{R2}$ in phase with the rotor current emulating the voltage drop over an external resistance. The rotor induced voltage $\underline{e}'_R$ in a squirrel cage machine is represented by the continuous line while the rotor induced voltage in a doubly-fed machine is increased by the higher slip values and represented by the dashed line. The voltage drops over the rotor complex impedance is depicted for each of these values.

One may assume the operating point number 1 as the original value for the machine with short-circuited rotor, i.e. $\underline{u}_{R1}$ = 0, by slip $\underline{s}_1$ and stator and rotor currents $\underline{i}_{S1}$ and $\underline{i}'_{R1}$, respectively. A positive increase in the rotor voltage to $\underline{u}'_{R0}$ forces the rotor current to a new value $\underline{i}'_{R0}$, according to (95) and the stator current to $\underline{i}_{S0}$, according to (47), as well as the

slip to s_0. It means that the speed is increased and a reduced voltage $s_0 \underline{e}_S$ is induced in the rotor circuit. Similarly, a negative increase in the rotor terminal voltage to $\underline{u}'_{R2}$ forces the rotor and stator currents to $\underline{i}'_{R2}$ and $\underline{i}_{S2}$, respectively. The speed is reduced and the induced voltage in the rotor side increases to $s_2 \underline{e}_S$. The fact that the rotor voltage and currents are in phase means that only active power is flowing between the controllable voltage source and the rotor circuit.

The dotted arcs point out the loci of the stator (Heyland circle) and rotor currents, taking the stator parameters into consideration. Furthermore, the internal stator's induced voltage and the magnetising current also deviate slightly from the assumed constant values due to the voltage drop over the stator winding. In comparison to the cage machine, the doublyfed induction machine possesses a family of Heyland circles, depending on the imposed rotor voltage. This degree of freedom allows for determining the current loci for desired slip values. The rotor voltage vector can be chosen in such a way as to ensure that only the imaginary components of the rotor and stator currents vary, as can be deduced from (95). In this case, machine magnetisation may be influenced independently of speed. The machine can be overand under-excited through the rotor circuit in the same way as a synchronous machine. Depending on the available ceiling voltage and on the operating point the machine may be fully magnetised through the rotor or even assume capacitive characteristics.

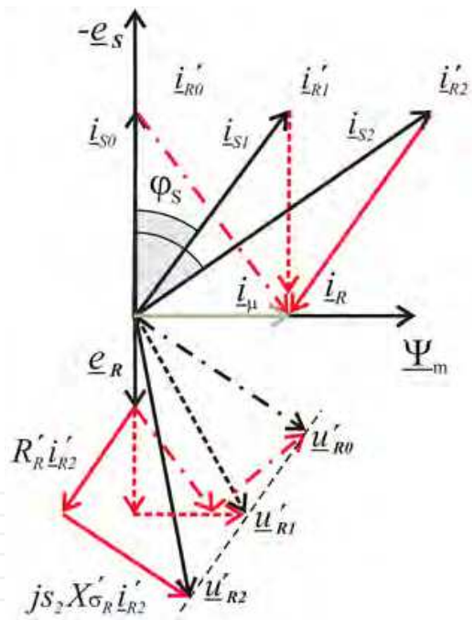

Fig. 6. Magnetisation between stator and rotor

The figure 6 shows this kind of operation for 3 distinct operating points, where the rotor voltages $\underline{u}'_{R0}$, $\underline{u}'_{R1}$ and $\underline{u}'_{R2}$ are applied to the rotor terminals in order to determine the way the machine is being magnetised. The real component of the currents is kept constant in order to maintain a constant torque or active power. The resulting stator and rotor current vectors for all situations according to (47) are also depicted. For the operating point 2, one notices that the rotor current is demagnetising so that the machine is under-excited. The imaginary component of the resulting stator current compensates the demagnetisation referring the required reactive power from the network. In situation 1 magnetisation is

carried out through the stator circuit and the rotor current vector is aligned with the internal induced voltage. In the case 0, the rotor current assumes the magnetising current. The resulting stator current possesses only a real component and the stator power factor equals one. If the rotor voltage angle is further increased in this direction the machine will be over-excited and the imaginary component of the stator current will be capacitive.

4. LC-Filter and mains supply

The basic electrical circuits theory is used in modeling the LC-filter and the mains supply at the output of the mains side inverter. Initially, the inverter and the mains are considered ideal symmetrical 3-phase voltage sources, $\underline{u}_n$ and $\underline{u}_N$, respectively. The LC-filter composed of the filter inductance and capacitance, L_f and C_f, together with the filter resistance R_f, build the first mesh. The network impedance $\underline{Z}_N = R_N + j\omega_N L_N$ between the capacitor filter and the mains voltage source builds the second mesh. Lastly, one gets a T-circuit that is similar to the induction machine equivalent circuit, but instead of a magnetising inductance the filter capacitance as shown in figure 7.

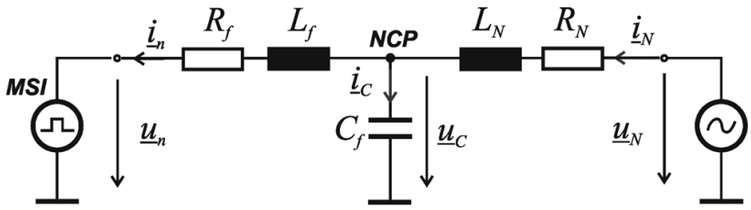

Fig. 7. LC-filter and mains supply equivalent circuit

4.1 Steady state analysis

Considering the equivalent circuit 7, the steady state voltage and current equations of the LC-filter and of the mains supply can be written as

$$\underline{u}_C = R_f \underline{i}_n + jX_f \underline{i}_n + \underline{u}_n \tag{97}$$

$$\underline{u}_N = R_N \underline{i}_N + jX_N \underline{i}_N + \underline{u}_C \tag{98}$$

$$\underline{i}_C = j\frac{\underline{u}_C}{X_C} = \underline{i}_N - \underline{i}_n, \tag{99}$$

where $X_f = \omega_N L_f$, $X_N = \omega_N L_N$ and $X_C = \dfrac{1}{\omega_N C_f}$ are the respective inductive and capacitive reactances of the filter inductor, network and filter capacitor.

If one neglects the voltage drop over the mains impedance, the voltage over the capacitor becomes equal to the net voltage. Under this assumption voltage equations above can be simplified to

$$\underline{u}_N = R_f \underline{i}_n + jX_f \underline{i}_n + \underline{u}_n \tag{100}$$

$$\underline{u}_N = \underline{u}_C \tag{101}$$

4.1.1 Active power flow.

The power flowing from the network to the MSI output can be computed as it was for the generator side using expressions (41) and (42) in equation (100). The active power is given by

$$p_n = \frac{3}{2}\Re\{\underline{u}_N \underline{i}_n^*\} = \frac{3}{2}\Re\{R_f \underline{i}_n \underline{i}_n^* + jX_f \underline{i}_n \underline{i}_n^* + \underline{u}_n \underline{i}_n^*\}. \tag{102}$$

The active power flowing at the net connecting point (NCP) is composed of the power losses in the filter resistance

$$P_{Cu_f} = \frac{3}{2} R_f \hat{I}_n^2, \tag{103}$$

and the contribution of the mains-side inverter (MSI) measured at its output

$$p_n' = \frac{3}{2}\Re\{\underline{u}_n \underline{i}_n^*\}. \tag{104}$$

Based on expression (99) and the fact that the capacitor filter current presents no active component, one may conclude that the active current components of the inverter and network must be the same. Hence, the active power flowing to or from the network is equal the active power being delivered at the NCP in equation (102) and is given as

$$p_N = \frac{3}{2}\Re\{\underline{u}_N \underline{i}_N^*\} = \frac{3}{2}\Re\{\underline{u}_N \underline{i}_n^*\} = p_n. \tag{105}$$

4.1.2 Reactive power flow.

The reactive power at NCP is the remaining imaginary part of (102)

$$q_n = \frac{3}{2}\Im\{\underline{u}_N \underline{i}_n^*\}, \tag{106}$$

consisting of the contribution of the inductor filter

$$Q_L = \frac{3}{2} X_f \hat{I}_n^2, \tag{107}$$

and the inverter's reactive power contribution

$$q_n' = \frac{3}{2}\Im\{\underline{u}_n \underline{i}_n^*\}. \tag{108}$$

The capacitor contribution is purely reactive and can be easily computed as

$$q_C = \frac{3}{2}\Im\{\underline{u}_N \underline{i}_C^*\}, \tag{109}$$

where the current flowing through the capacitor is given by (99). Developing (109) yields

$$Q_C = -\frac{3}{2}\frac{\hat{U}_N^2}{X_C}, \tag{110}$$

The *LC*-filter reactive power share due to its passive components, namely the inductor and capacitor, can be summarised by the following expression

$$Q_F = Q_L + Q_C = \frac{3}{2} X_f \hat{I}_n^2 - \frac{3}{2} \frac{\hat{U}_N^2}{X_C} \cdot \tag{111}$$

The total reactive power flowing to or from the network can be computed as

$$q_N = \frac{3}{2} \Im\{\underline{u}_N \underline{i}_N^*\} \cdot \tag{112}$$

Once again taking equation (99) and remembering that the capacitor current possesses only a reactive component, the total reactive current is composed by the MSI and the filter capacitor's reactive current components.
Substituting the current relation in (112) and using the relations pointed out in the reactive power expressions above, one may see that the total reactive power is composed by MSI and *LC*-filter contributions

$$q_N = \frac{3}{2} \Im\{\underline{u}_N (\underline{i}_n + \underline{i}_C)^*\} \Rightarrow q_N = q_n + q_C \cdot \tag{113}$$

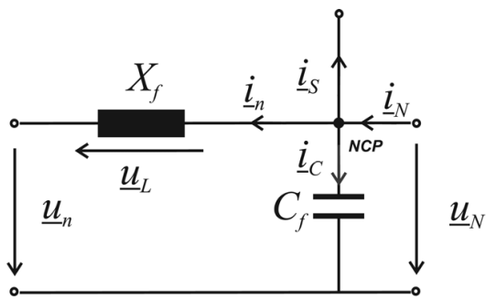

Fig. 8. LC-filter and mains supply equivalent circuit

4.1.3 Generator contribution.

If the DFIG stator terminals are connected to the NCP as shown in the equivalent circuit in figure 8, one has to newly compute the power flow balance. Let us now consider the stator current flowing from the NCP node. According to Kirchoff current's law the node equation is then

$$\underline{i}_N = \underline{i}_C + \underline{i}_n + \underline{i}_S \cdot \tag{114}$$

The active and reactive powers being delivered to the network in this situation can be easily computed substituting expression (114) in the equations (105) and (112), respectively. If we develop this equation further, based on the considerations made on the capacitor current and the power expressions derived in this section, we have

$$p_N = \frac{3}{2} \Re\{\underline{u}_N (\underline{i}_n + \underline{i}_S)^*\} = p_n + p_S \cdot \tag{115}$$

$$q_N = \frac{3}{2}\Im\{\underline{u}_N(\underline{i}_C + \underline{i}_n + \underline{i}_S)^*\} = q_C + q_n + q_S \cdot \tag{116}$$

Both these equations are very important in fostering further development of the optimization procedures in the next chapters.

4.1.4 Simplified analysis.

For a better understanding of the MSI operation together with the output LC-filter, some simplifications are featured. The first is the above-mentioned consideration that the capacitor is constant and equal the net voltage. The second is to neglect the filter resistance as shown in the simplified equivalent circuit in figure 8. Under these assumptions and according to the equivalent circuit, the voltage difference between the converter output and the net voltage is the voltage drop over the filter inductance

$$\underline{u}_n = \underline{u}_N - \underline{u}_L = \underline{u}_N - jX_f\underline{i}_n \cdot \tag{117}$$

If one orients the reference coordinate system oriented to the net voltage space vector and vary the active current component, active power can be delivered to or consumed from the network by MSI. According to (117) the voltage drop over the filter inductance is always in quadrature with the mains voltage, if the inverter output current is in phase with it, i.e., $\underline{i}_n$ possesses only a real part

$$\underline{u}_L = jX_f\underline{i}_n \cdot \tag{118}$$

The MSI output voltage $\underline{u}_n$ required to impose the output current can thus be determined. This situation is depicted in left figure 9.

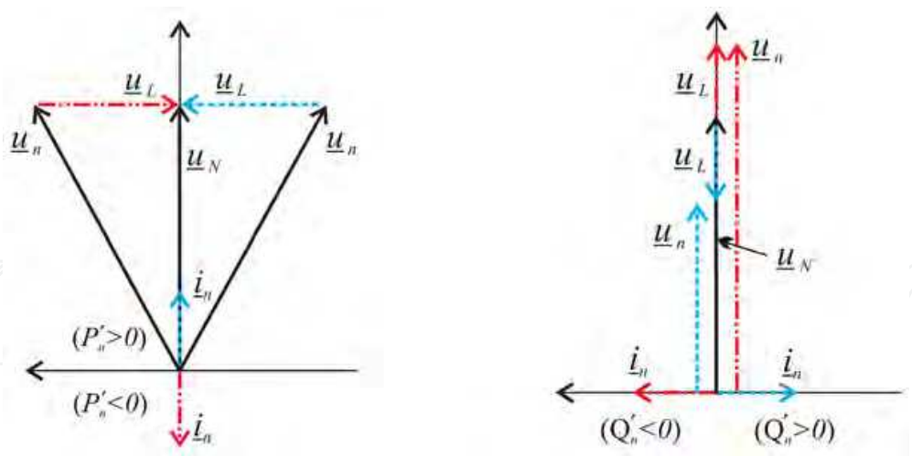

(a) Active Current (b) Reactive Current

Fig. 9. Phasor diagram for active (a) and reactive (b) currents

According to equation (104) the active power production or consumption, i.e., whether negative or positive, depends on the active current component's sign.

For the disconnected generator stator, where $\underline{i}_S$ =0, substituting (117) in (104) and considering that no active power can be produced or consumed by the inductor, the active power at the MSI is equal to the active power in the network .

$$p'_n = \frac{3}{2}\Re\{(\underline{u}_N - \underline{u}_L)\underline{i}_n^*\} = \frac{3}{2}\Re\{\underline{u}_N\underline{i}_n^* - \underline{u}_L\underline{i}_n^*)\} = p_N\,, \tag{119}$$

Allowing the reactive current to vary in the quadrature axis results in voltage drops over the filter inductor parallel to the net voltage, whose sense depends on that of the current. The required inverter output voltages in order to impose these currents are in phase with the mains voltage vector and can be computed based on (117). Since the active current component is zero, the reactive power production or consumption, i.e., negative or positive, depends on the sign of the reactive current component, as per (108). The phasor diagram for this situation is found in right figure 9.
Again considering the disconnected generator, if one substitutes (117) in (108), we have the expression

$$q'_n = \frac{3}{2}\Im\{(\underline{u}_N - \underline{u}_L)\underline{i}_n^*\} = q_n - q_L\,. \tag{120}$$

Hence, besides the capability to deliver and consume active power, the MSI is able to work as a static synchronous compensator or a phase shifter, influencing the net voltage and the power factor in order to produce or consume reactive power. Equation (119) and (120) can be used for the design of the MSI.

5. System topology and steady state power flow

The common DFIG drive topology depicted in figure 10 shows the stator directly connected to the mains supply while the rotor is connected to the rotor-side inverter. A voltage DC-link between the rotor and mains-side inverter performs the short-term energy storage between the generator rotor and the network. The LC-filter at the MSI output damps the harmonic content of the output voltage and current. The bi-directional converters, i.e., inverter/rectifier operation, enable the active and reactive power flow in both directions. Within the sub-synchronous speed range, the active power flows from the grid to the rotor circuit whereas within the super-synchronous speed range, it flows from the rotor to the grid. The sub-syncrhonous operation mode is illustrated in figure 11.

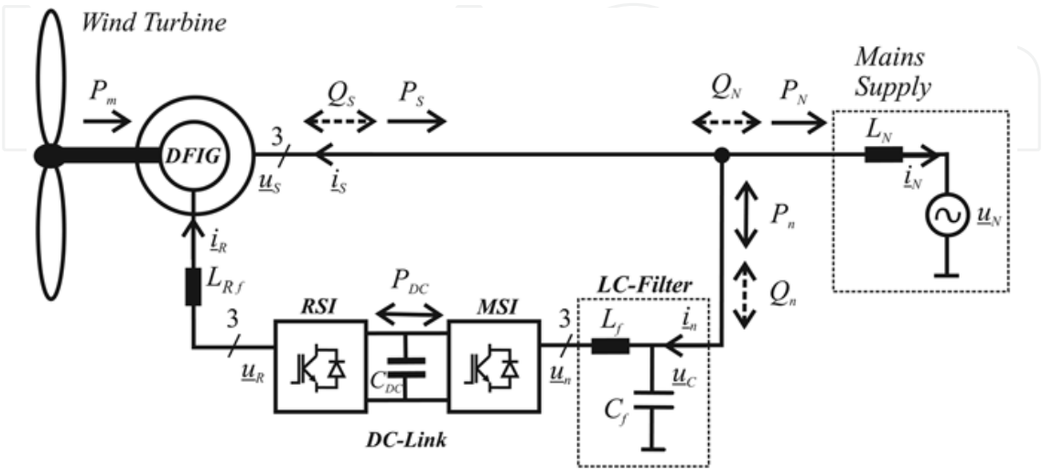

Fig. 10. 3-phase schematic

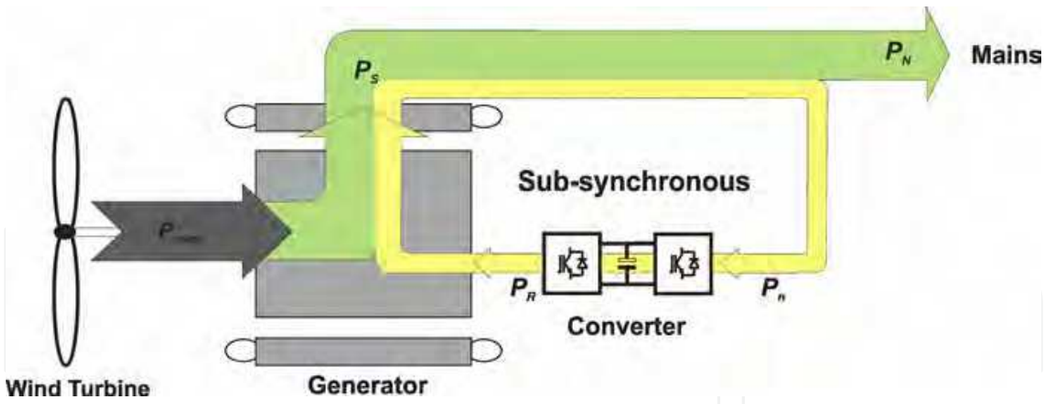

Fig. 11. Active power flow in sub-synchronous operation

5.1 Active power flow

The active power P_R flowing through the rotor circuit, also named slip power, is proportional to stator active power P_S and to the slip s, as denoted by expression (75). Neglecting the copper losses, the slip relation becomes

$$P_R = -sP_S \cdot \tag{121}$$

For a constant DC-link voltage U_{DC}, neglecting the losses in the converter, the output power in the MSI P_n must be equal the rotor power, thereby guaranteeing the energy balance

$$P_n = P_R \cdot \tag{122}$$

The total active power delivered to the network P_N is the sum of the stator power plus the MSI output power at the net connecting point.

$$P_N = P_S + P_n \cdot \tag{123}$$

Now, substituting (121) and (122) in (123) yields

$$P_N = (1-s)P_S \cdot \tag{124}$$

5.2 Reactive power flow

From equation (84) and the simplifications assumed for the equivalent circuit depicted in figure 4, the required reactive power Q_m to be delivered to the generator for the rated magnetization can be found as

$$Q_m = \frac{3}{2}\frac{\hat{U}_S^2}{X_m} \cdot \tag{125}$$

Besides controlling the active power flow, the bi-directional switches on the inverters enable the phase displacement between converter output current and voltage allowing for the generation or consumption of reactive power, as shown in figure 12. Therefore, the machine excitation can be also carried out through the rotor circuit so that Q_m can be delivered by the stator, rotor, mains supply and the RSI. According to equation (92), neglecting the leakage reactive powers, the following expression can be written for the magnetising reactive power

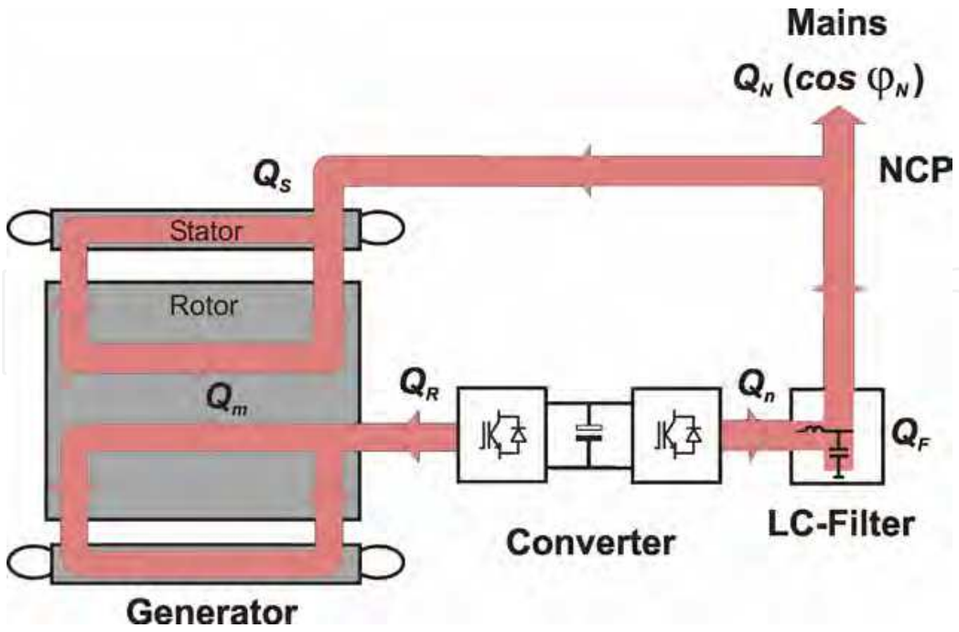

Fig. 12. Reactive power flow

$$Q_m = Q_S - \frac{Q_R}{s} \Rightarrow Q_S = Q_m + \frac{Q_R}{s}. \tag{126}$$

The equation (126) above shows how the reactive power in the stator side can be determined by the reactive power fed to the rotor side and influences the stator power factor. It also points out the required values for the rotor reactive power in order to impose unity power factor to the stator side

$$Q_S = 0 \Rightarrow Q_R = -sQ_m. \tag{127}$$

In this way the full machine magnetisation is accomplished by the rotor side. Also capacitive (leading) power factors can be imposed to the stator terminals provided that

$$Q_R < -sQ_m. \tag{128}$$

Hence, the dimensioning of the inverter depends also on the desired power factor control range and has to be extended in order to accommodate the additional reactive power that flows through the rotor circuit. This is also true for the MSI if power factor correction or voltage regulation is required.

The reactive power contributions to the MSI Q_n and to the LC-filter capacitance Q_C can be also taken into account and influence the power factor in the NCP.

The total reactive power delivered to or consumed by the network Q_N at the NCP is given by the addition of the DFIG stator, MSI and LC-filter contributions, as pointed out in expression (116).

Substituting the stator reactive power given by equation (126) yields

$$Q_N = Q_C + Q_n + Q_m + \frac{Q_R}{s}, \tag{129}$$

where Q_R and Q_n are available controllable reactive powers. Choosing the filter capacitance in order to compensate the generator power factor, i.e. $Q_C = -Q_m$ expression (129) is reduced

$$Q_N = Q_n + \frac{Q_R}{s}. \tag{130}$$

On the other hand, using a simple L-filter gives

$$Q_N = Q_n + Q_m + \frac{Q_R}{s}, \tag{131}$$

With the derived equations for the active and reactive power flow capability diagrams for the DFIG drive can be drawn as it was carried out in Santos-Martin et al. (2008) including the contribution of the mains-side inverter and LC-filter.

The possibility of distributing the reactive power between stator and rotor allows for the splitting of the magnetising current in stator and rotor reactive current components. Depending on the operating point, i.e., on the active currents and on the winding resistances, the reactive current may be smartly distributed so as to reduce system losses.

The optimisation of the power flow aims to reduce inherent losses with a view to improving drive efficiency. The efficiency can be determined by computing the power losses corresponding to the amount of energy that is transformed into heat during the conversion process. In an electrical drive, losses are present as electrical losses due to the current flowing through the involved circuits and to semiconductors switching in the inverter, as iron losses in the magnetic circuit of the electrical machine, transformer and filter cores, and as mechanical losses due to friction and windage. Hence, the problem consists in minimising the losses by manipulating one or more optimisation variables. The required control structure and controllers design in order to perform the reactive power splitting is described in Rabelo et al. (2009).

6. Conclusion

The basics of electrical drives in rotating *dq*-coordinate system was introduced as well as the classical definition of active and reactive powers leading to the complex power. Electrical power generation, specifically the induction generator and later the doubly-fed induction machine and the power flow were discussed. The simplified analysis showed the possible operating ranges of the doubly-fed induction generator drive for production of active and reactive powers.

The drive system topology allows for an independent control of the reactive power in the generator and mains side as well as the decoupling from the active power due to the mains voltage or flux orientation. The suggested optimisation is based on the controlled distribution of the reactive power flow in the drive components. The reactive power can be defined the rate of magnetic and electrical energy exchange between the generator, the mains supply and the inverters. It is a function of the reactive current and of the voltage amplitude and, therefore, closely related to process losses. For this reason, it proves to be a very suitable optimization variable.

7. References

Leonhard, W. (1980). *Regelung in der elektrischen Energieversorgung*, 6th edn, B.G. Teubner, Stuttgart.

Lipo, T. (1995). *Vector Control of Electrical Machines*, 1st edn, Clarendon Press, Clarendon.

Müller, G. (1977). *Elektrische Maschinen - Theorie rotierender elektrischer Maschinen*, 4th edn, VEB Verlag Technik, Berlin.

Rabelo, B. & Hofmann, W. (2002). Optimal reactive power splitting with the doubly-fed induction generator for wind turbines, *DEWEK Conference Proceedings*, Wilhemshaven.

Rabelo, B., Hofmann, W., Silva, J., Gaiba, R. & Silva, S. (2009). Reactive power control design in doubly-fed induction generators for wind turbines, *IEEE Transactions on Industrial Electronics* . Vol.56, No.10, pp.4154-4162, October 2009.

Rabelo, B., Hofmann,W., Tilscher, M. & Basteck, A. (2004). A new topology for high powered wind energy converters, *EPE PEMC Conference Proceedings*, Riga.

Santos-Martin, D., Arnaltes, S. & Amenedo, J. R. (2008). Reactive power capability of doubly-fed asynchronous generators, *ELSEVIER Electric Power Systems Research*. Vol.78, Issue 11, pp.1837-1840, November 2008.

Späth, H. (2000). *Leistungsbegriffe für Ein- und Mehrphasensysteme*, 1st edn, VDE Verlag, Berlin, Offenbach.

Vicatos, M. & Tegopoulos, J. (1989). Steady state analysis of a doubly-fed induction generator under synchronous operation, *IEEE Transactions on Energy Conversion* . Vol.4, No.3, pp.495-501, 1989.

Wechselstromgrössen - Zweileiter Stromkreise (1994). Din norm 40110 teil 1, Deutsches Institut für Normung.

Wind Power

Edited by S M Muyeen

ISBN 978-953-7619-81-7
Hard cover, 558 pages
Publisher InTech
Published online 01, June, 2010
Published in print edition June, 2010

This book is the result of inspirations and contributions from many researchers of different fields. A wide verity of research results are merged together to make this book useful for students and researchers who will take contribution for further development of the existing technology. I hope you will enjoy the book, so that my effort to bringing it together for you will be successful. In my capacity, as the Editor of this book, I would like to thanks and appreciate the chapter authors, who ensured the quality of the material as well as submitting their best works. Most of the results presented in to the book have already been published on international journals and appreciated in many international conferences.

How to reference

In order to correctly reference this scholarly work, feel free to copy and paste the following:

Balduino Rabelo and Wilfried Hofmann (2010). Doubly-fed Induction Generator Drives for Wind Power Plants, Wind Power, S M Muyeen (Ed.), ISBN: 978-953-7619-81-7, InTech, Available from: http://www.intechopen.com/books/wind-power/doubly-fed-induction-generator-drives-for-wind-power-plants

INTECH
open science | open minds

InTech Europe
University Campus STeP Ri
Slavka Krautzeka 83/A
51000 Rijeka, Croatia
Phone: +385 (51) 770 447
Fax: +385 (51) 686 166
www.intechopen.com

InTech China
Unit 405, Office Block, Hotel Equatorial Shanghai
No.65, Yan An Road (West), Shanghai, 200040, China
中国上海市延安西路65号上海国际贵都大饭店办公楼405单元
Phone: +86-21-62489820
Fax: +86-21-62489821

IntechOpen